Abstract No. 10IKC–32

PETROLOGY OF LAMPROITES FROM THE NUAPADA LAMPROITE FIELD, BASTAR CRATON, INDIA

Sahu[*] N[1], Gupta T[2], Patel SC[2], Khuntia DBK[2], Thakur SS[3] and Das SK[1]

[1] *Directorate of Geology, Government of Odisha, Bhuvigyan Bhawan, Bhubaneshwar 751001, India*

[2] *Department of Earth Sciences, Indian Institute of Technology, Bombay, Powai, Mumbai 400076, India*

[3] *Wadia Institute of Himalayan Geology, 33 Gen. Mahadev Singh Road, Dehradun 248 001, India*

[*]***Email:*** *narottam1960@gmail.com*

Introduction

Kimberlites and lamproites in India are known to occur in the Dharwar Craton, Bastar Craton and Bundelkhand Craton (Fig. 1). These cratons are Archaean terranes comprising quartzofeldspathic gneisses and granitoids with Proterozoic platformal cover sequences in several parts. Kimberlites and lamproites in the Bastar Craton are confined to its eastern part near the contact with the Proterozoic Eastern Ghats Mobile Belt.

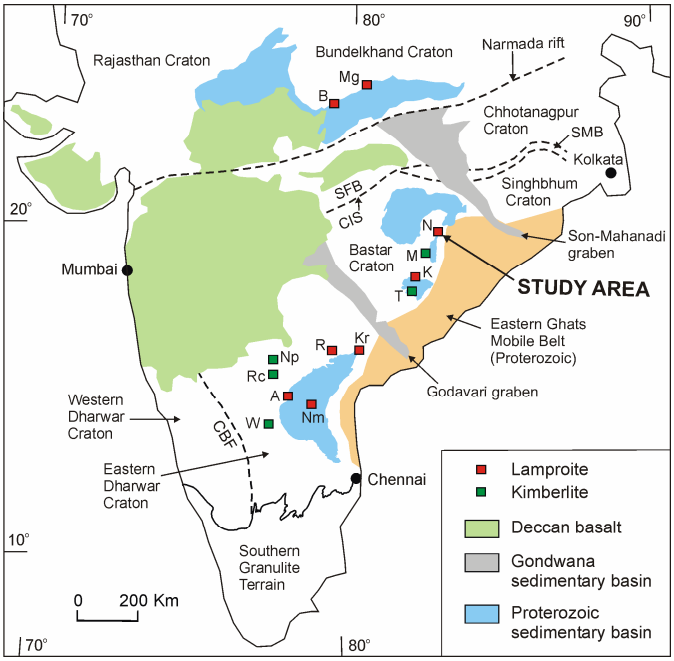

Fig.1. Schematic geological map of India. CBF – Chitradurga Boundary Fault; CIS – Central India Shear Zone; SFB – Satpura Fold Belt; SMB – Singhbhum Mobile Belt; A – Aliabad; B – Bunder; K – Khadka; Kr – Krishna; M – Mainpur; Mg – Majhgawan; N – Nuapada; Nm – Nallamalai; Np – Narayanpet; R – Ramadugu; Rc – Raichur; T – Tokapal; W – Wajrakarur.

Kimberlites of the Bastar Craton are distributed in two fields, viz. Mainpur Kimberlite Field (MKF, diamondiferous), and Tokapal Kimberlite Field (barren). The MKF has six intrusions, while the TKF has two intrusions. Lamproites are known from two areas in the Bastar Craton, viz. Nuapada in Odisha and Khadka in Chhattisgarh. The Nuapada Lamproite Field (NLF) contains hypabyssal facies lamproite dykes at Kalmidadar and Darlimunda, and lamprophyre dykes at Amlidadar, Parkom and Darlimunda. The objectives of the present study are to: (i) examine the major element composition of mantle-derived spinel and garnet recovered from stream sediments and soil samples in the Kalmidadar area; and (ii) give the first mineralogical and geochemical data on the lamproites and lamprophyres of the NLF.

Nuapada Lamproite Field

The NLF is dominantly occupied by two types of Precambrian granitoids, viz. an older grey granitoid (weakly foliated) (~ 2550 My old), and a younger pink granitoid (unfoliated) (Fig. 2). The latter occupies the western part of the area and locally contains blocks of grey granite. Neoproterozoic platformal cover rocks of the Khariar basin are exposed in the southern part of the area and include sandstone (Devdahra Sandstone) and shale (Kulharighat Formation) of the Pairi Group.

The Kalmidadar lamproite (KD) (82° 22′ 20″ : 20° 45′ 10″) is a diamondiferous, N–S trending, elongate body with surface dimension of ~ 320 m × 160 m. It is completely weathered at the surface and weathering is persistent up to a depth of 12 m or more as revealed by drill cores. Its diamond grade is 9.95 cpht. The Darlimunda lamproite is a dyke swarm comprising several, mostly N–S trending dykes marked by isolated, patchy hardebank exposures. Mukhopadhyay et al. (2004) considered the isolated exposures as individual dykes of lamproite and reported eight such dykes (I to VIII) in the Darlimunda area. However, our work shows that many of these small discontinuous exposures constitute parts of larger dyke systems. Furthermore, the dykes I and II of Mukhopadhyay et al. (2004) are not lamproites. While dyke I is a lamprohyre, dyke II is neither a lamproite nor a

10th IKC

lamprophyre. We have grouped the dykes III to VIII of Mukhopadhyay et al. (2004) into two lamproite dyke systems (DM1 and DM2). The DM1 lamproite (20° 50′ 10″N : 82° 38′ 20″E) is a broadly N–S trending dyke with ~ 5 m × 150 m size. Near the southern end of this dyke, a small, NE–SW trending dyke (20° 50′ 09″N : 82° 38′ 13″E) of ~ 2 m × 20 m size occurs. This small dyke corresponds to the dyke VI, whereas the main DM1 dyke includes the dykes VII and VIII of Mukhopadhyay et al. (2004). The DM2 lamproite (20° 50′ 00″N : 82° 38′ 32″E) is a broadly N–S trending dyke with an average width of ~ 5 m and length of ~ 130 m. Hardebank outcrops are patchy and sparse in this dyke and the granitoid country rock is veined by thin, irregular apophyses of lamproite originating from the main intrusion. This intrusion includes the dykes III, IV and V of Mukhopadhyay et al. (2004).

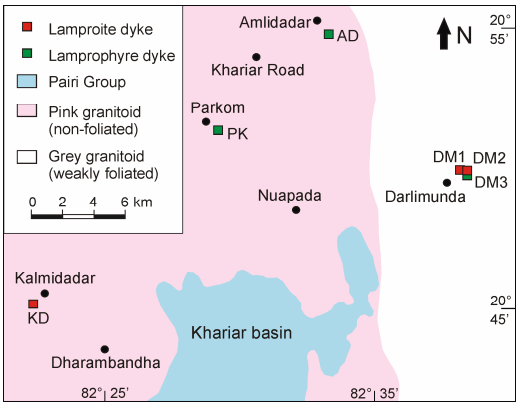

Fig.2. Generalised geological map of Nuapada Lamproite Field. AD – Amlidadar; DM – Darlimunda; KD – Kalmidadar; PK – Parkom.

The dyke I of Mukhopadhyay et al. (2004) is named here DM3 lamprophyre (20° 49′ 54″N : 82° 38′ 22″E), which exhibits an E–W trend with ~ 3 m × 25 m size. The Amlidadar lamprophyre (AD) (20° 54′ 52″N : 82° 33′ 11″E) is a N–S trending dyke of ~ 1 m × 40 m size. The Parkom lamprophyre (PK) (20° 51′ 32″N : 82° 29′ 11″E) is a thin (0.5 m wide), N–S trending dyke of 15 m length. The dykes AD and PK correspond to the dykes IX and X, respectively of Mukhopadhyay et al. (2004), who considered these bodies as lamproites. However, our mineralogical study shows that these bodies are not lamproites. A mafic dyke at Sakri, reported by Shrivastava et al. (2002) as lamproite, has been found to be dolerite.

Age of Nuapada lamproites

Whole rock Ar–Ar isotopic analysis of two samples, one each from the Kalmidadar and Darlimunda lamproites, was carried out by Thermo Fischer Scientific ARGUS-VI Mass Spectrometer at the Indian Institute of Technology, Bombay. Both the rocks yielded saddled-shaped patterns with a plateau age of 1030 ± 20 My. This represents the crystallisation age of the lamproites which assumes significance in view of the fact that Lehmann et al. (2010) dated two kimberlites of the MKF as 65 My old.

Indicator mineral chemistry

Gravel samples collected during regional indicator mineral survey and soil samples collected during detailed survey were processed for recovery of heavy minerals. Cr-spinel was abundant in the intermediate magnetic fraction, whereas garnet was occasionally found in the non-magnetic fraction. Picroilmenite and Cr-diopside were not found in any of the samples. Cr-spinel grains are elongated to subrounded in shape with beveled edges and exhibit concave fracture and micropitted surface. They appear fresh worn to worn. Garnet grains are purple to wine-red in colour with frosted to scaly frosted surface. They exhibit strong internal colour change (firing) and subconchoidal fracture.

This study examines the compositions of 54 spinels and 9 garnets from the indicator mineral suite on and around Kalmidadar lamproite. The minerals were analyzed by Oxford ISIS EDS attached to a JEOL6400 SEM at the Centre for Microscopy Characterisation and Analysis, University of Western Australia, Crawley, Western Australia.

The Kalmidadar Cr-spinels show wide variations in Cr_2O_3 (33–67 wt%, mostly above 50 wt%), Al_2O_3 (5–38 wt%.), MgO (11–18 wt%) and FeO^T (9–20 wt%). They have low TiO_2 content (< 1 wt%) except for a few grains with up to 2.4 wt% TiO_2. Stoichiometric calculations yield very low ferric iron in the Cr-spinels with $Fe^{3+}/(Cr+Al+Fe^{3+})$ ratios below 0.06. Their X_{Mg} (= $Mg/Mg+Fe^{2+}$) ratio falls in the range of 0.49–0.77, while the Cr# [= Cr/(Cr+Al)] varies from 0.52 to 0.91 except for a few grains with values between 0.38–0.48. Majority of the Cr-spinel population can be classified as Ti-poor, aluminous magnesiochromite. In the MgO–Cr_2O_3 plot the Kalmidadar Cr-spinels exhibit a negatively sloping trend and extend into the diamond inclusion field consistent with their diamondiferous association (Fig. 3). On a plot of Cr/(Cr+Al) vs $Fe^{2+}/(Mg+Fe^{2+})$, the Cr-spinels show an overall tendency of increasing Cr-number with increasing $Fe^{2+}/(Mg+Fe^{2+})$ (Fig. 4). This trend, known as the Cr–Al trend, could be a high- to low-pressure trend if spinel compositions in mantle peridotitic source were controlled by Al–exchange with coexisting pyroxenes (Barnes and Roeder, 2001).

The Kalmidadar garnets have Mg# [= $Mg/(Mg+Fe^T)$] in a narrow range of 0.83–0.88. Their Cr_2O_3 content varies significantly between 1.4–7.2 wt%, while the CaO content falls in the range of 4.6–6.1 wt%. In the MgO–CaO–Cr_2O_3 diagram the Kalmidadar pyropes fall in the G9 (lherzolitic garnet) field (Fig. 5). On Cr_2O_3 vs CaO plot, the pyropes follow the typical lherzolitic trend, which reveals that the garnets were derived from a lherzolitic mantle source (Fig. 6).

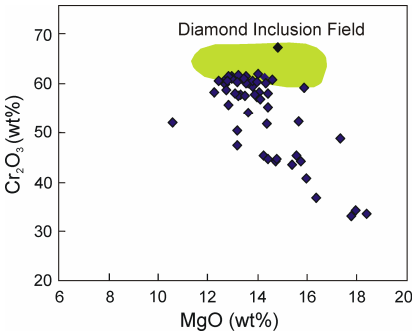

Fig.3. MgO–Cr_2O_3 plot of Kalmidadar Cr-spinels. Diamond inclusion field after Fipke et al. (1995).

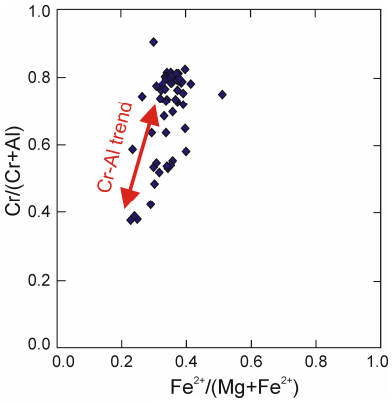

Fig.4. Kalmidadar Cr-spinels on Cr/(Cr +Al) vs $Fe^{2+}/(Mg+Fe^{2+})$ diagram.

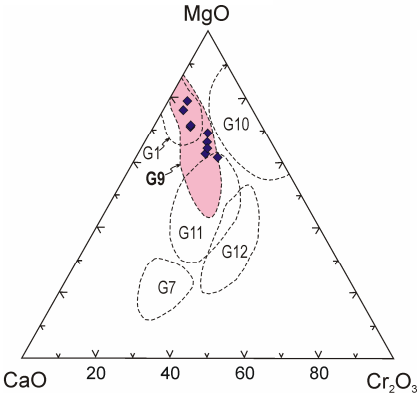

Fig.5. MgO–CaO–Cr_2O_3 plot of Kalmidadar garnets. Fields after Dawson and Stephens (1975).

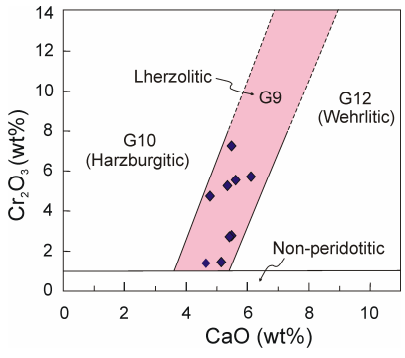

Fig.6. Kalmidadar garnets on CaO vs Cr_2O_3 plot. Fields of harzburgitic, lherzolitic and wehrlitic garnets after Grutter et al. (2004).

Mantle phase equilibria considerations show that the subsolidus transition of spinel peridotite to garnet peridotite occurs via the generalised reaction: spinel + pyroxene(s) = garnet + olivine. In the chemical system MgO–Al_2O_3–Cr_2O_3–SiO_2, a pressure–temperature field exists where garnet and spinel coexist. The width of this divariant field strongly depends on the Cr/(Cr+Al) of the system, and with increasing value of this ratio the spinel–garnet transition progressively shifts to pressures as high as ~ 70 kbar (i.e., depth of ~ 200 km) (Klemme, 2004). From the high Cr# of Kalmidadar Cr-spinels, it can be said that they are derived from sources as deep as 200 km.

Mineralogy of lamproites and lamprophyres

Since the Kalmidadar lamproite is completely weathered at the surface, the studied samples are from bore holes (up to 30 m depth) drilled by the Directorate of Geology, Government of Odisha. Samples from all other bodies are from surface exposures. Mineralogically, the Kalmidadar lamproite comprises phenocrysts (0.5–1 mm) of olivine (pseudomorphed by calcite and talc) and microphenocrysts (0.1–0.3 mm) of phlogopite set in a groundmass of secondary chlorite and calcite (Fig. 7). The Darlimunda lamproites (DM1 and DM2) have undergone pervasive hydrothermal and/or deuteric alteration, which has resulted in complete chloritisation of phlogopite microcrysts and groundmass flakes and extensive silicification of the rocks. Phenocrysts of olivine in the Darlimunda lamproites are mostly pseudomorphed by quartz. However, relicts of the primary textures are well-preserved thereby providing important clues to the mineralogy and nature of the protolith. Tiny grains of rutile and apatite are commonly scattered in the groundmass of both Kalmidadar and Darlimunda lamproites. Rutile often occurs as relict within silicified micro-nodules of variable TiO_2–SiO_2 composition. A rare subhedral grain of zircon (0.25 mm long) was observed in a slide of Kamlidadar lamproite. Microcrysts of titanite occur locally in the Kalmidadar lamproite, but are common in the Darlimunda lamproites.

The Amlidadar lamprophyre is broadly similar in mineralogy to the Kalmidadar lamproite, except that: (i) mica is mostly biotite instead of phlogopite; (ii) secondary talc is absent; and (iii) secondary pyrite is present. The Parkom lamprophyre comprises phenocrysts of olivine (pseudomorphed by calcite) set in a groundmass of acicular diopside and flaky biotite. Diopside and phlogopite occasionally form phenocrysts and microphenocrysts, respectively in this rock.

Minerals in the lamproites and lamprophyres were analysed by Cameca SX–100 electron microprobe at the Wadia Institute of Himalayan Geology, Dehradun. Phlogopites in the Kalmidadar lamproite have a compositional range of 5.4–7.4 wt% TiO_2, 8.6–11.2 wt% Al_2O_3, 7.3–9.2 wt% FeO^T. Their Mg# falls in the range of 0.80–0.83 (Fig. 8). The range of Mg# in biotites of Amlidadar lamprophyre is 0.37–0.68, while that in biotites of Parkom lamprophyre is 0.27–0.44. The Ba content of Kalmidadar phlogopites and Parkom biotites is low (< 0.5 wt% BaO), whereas that of Amlidadar

biotites is relatively high (2–3.6 wt% BaO). Diopside in the Parkom lamprophyre is rich in both Al (2.7–4.4 wt% Al_2O_3) and Ti (2.6–3.9 wt% TiO_2), while its Na_2O content is low (< 0.5 wt%). Rutile in the lamproites and lamprophyres contains up to 2.6 wt% Nb_2O_5 and up to 0.5 wt% ZrO_2.

The Amlidadar and Parkom rocks are named lamprophyre instead of lamproite because their mica is biotite instead of phlogopite, and the Parkom diopside is Al-rich. Mineralogically, the Kalmidadar and Darlimunda lamproites range from olivine phlogopite lamproite to phlogopite lamproite.

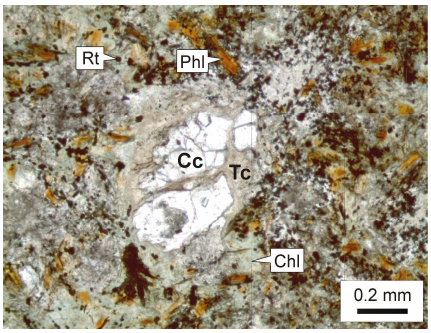

Fig.7. Photomicrograph of Kalmidadar lamproite under plane polarized light. Calcite (Cc) and talc (Tc) occur in pseudomorph after olivine phenocryst. Phlogopite (Phl) forms microphenocrysts. Groundmass comprises chlorite (Chl) and calcite with scattered grains of rutile (Rt), which is altered to TiO_2–SiO_2 micro-nodules.

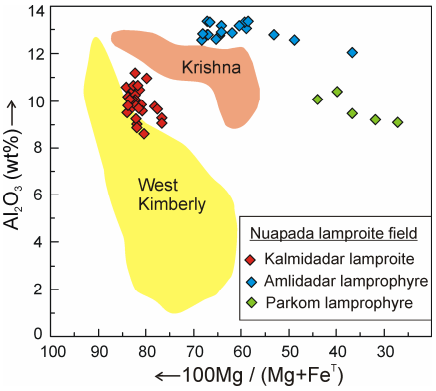

Fig.8. Compositional variation of mica in Nuapada lamproites and lamprophyres compared with that in Krishna lamproites, southern India (Reddy et al., 2003; Chalapathi Rao et al., 2010) and West Kimberly lamproites (Mitchell and Bergman, 1991 and references therein).

Mica grains in the Nuapada lamproites and lamprophyres often show chemical zoning marked by a narrow Fe-rich rim relative to the core. All the micas have appreciable tetraferric component since their (Si + Al) content is < 8 pfu (Fig. 9). Relationship between Ti content and octahedral site deficiency indicates two important substitution mechanisms in accommodating Ti in the micas, viz. Ti + □ ↔ 2Mg, and Ti + 2Al ↔ Mg + 2Si (Fig. 10). In terms of compositional range of phlogopite, the Kalmidadar lamproite is closer to the West Kimberly lamproites than to the Krishna lamproites.

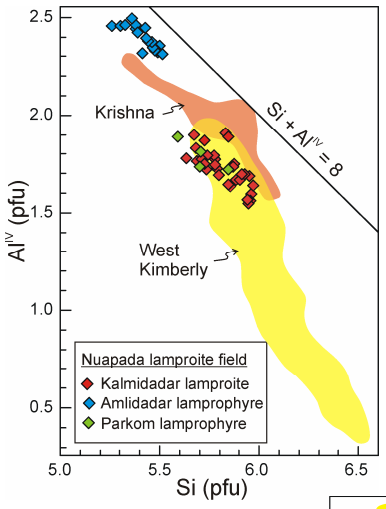

Fig.9. Tetrahedral Al vs Si plot for Nuapada micas. Data sources for compositional fields same as in Fig. 8.

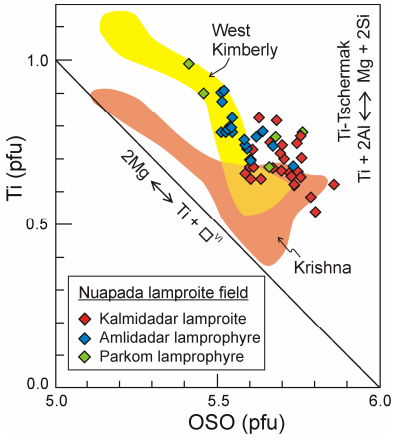

Fig.10. Nuapada micas on a plot of Ti vs Octahedral Site Occupancy (OSO). Data sources for compositional fields same as in Fig. 8.

Geochemistry

Bulk rock analyses of 5 samples of lamproites (2 from Kalmidadar and 3 from Darlimunda), and 3 samples of lamprophyres (1 each from Amlidadar, Parkom and Darlimunda) were carried out. Major elements and rare earth elements (preconcentrated via ion exchange resin), were analysed by Jobin Yvon Ultima–2 ICP–AES, and other trace elements by Phillips PW–2404 WD–XRF at the Indian Institute of Technology, Bombay.

The Nuapada lamproites have variable SiO_2 (44–60 wt%) content with higher values observed in rocks that are more silicified. The K_2O content of the rocks is generally low (< 0.4 wt%), which is attributed to chloritisation of phlogopite and consequent loss of K_2O to a hydrothermal fluid. The highest value of K_2O (1.34 wt%) is observed in a borehole sample from the Kalmidadar lamproite, which is rich in unaltered

phlogopite. The Nuapada lamproites have highly variable contents of MgO (7.4–14.3 wt%), FeO^T (7.2–11.1 wt%), CaO (2.2–12.3 wt%), TiO_2 (2.6–7.4 wt%) and P_2O_5 (0.1–1.9 wt%), while their Al_2O_3 content falls within a narrow range of 5.3–7.2 wt%. The lamprophyres have similar ranges of SiO_2, Al_2O_3, CaO, TiO_2 and P_2O_5 as the lamproites, but are richer in FeO^T (14.6–17.2 wt%), while having relatively low but uniform value of MgO (~ 8.7 wt%). Their K_2O content is low except for the Parkom lamprophyre (2.7 wt% K_2O), which is rich in unaltered phlogopite.

The Nuapada lamproites have high contents of compatible elements such as V (215–347 ppm), Cr (257–478 ppm) and Ni (232–423 ppm) as well as of incompatible elements such as Ba (2292–3499 ppm), Zr (544–780 ppm), Nb (52–135 ppm) and Hf (13–19 ppm). Zr and Hf behave coherently with an average Zr/Hf ratio of 42. The lamproites show high abundance of REE (∑REE = 790–1335 ppm) and enrichment in LREE relative to HREE [$(La/Yb)_N$ = 34–108] (Fig. 11A).

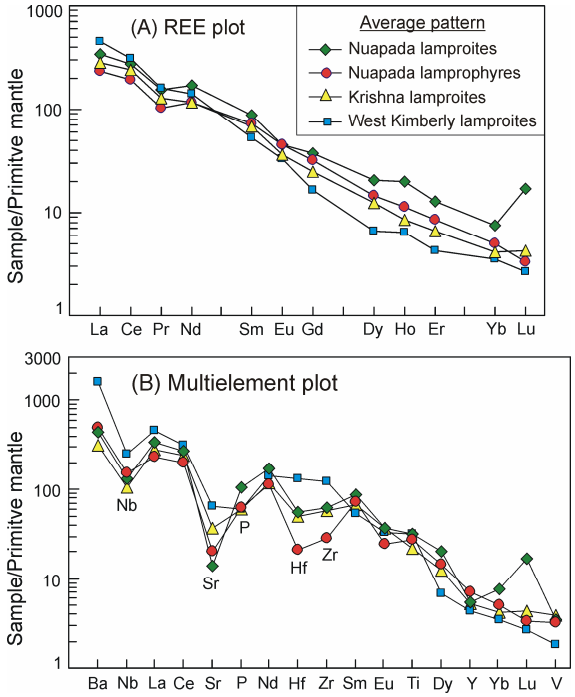

Fig.11. Primitive mantle normalised patterns of (A) rare earth elements and (B) multielements, in average Nuapada lamproite and average Nuapada lamprophyre compared with those of average Krishna lamproite (Vijesh, 2010) and average West Kimberly lamproite (Mitchell and Bergman, 1991 and references therein).

The Nuapada lamprophyres have similar contents of V, Cr, Ba and Nb as the lamproites, but are relatively poor in Ni (166–221 ppm), Zr (218–349 ppm) and Hf (4–9 ppm). Both the lamproites and lamprophyres usually have low Rb content (< 13 ppm), which correlates well with their low K_2O content that was caused by chloritisation of phlogopite. The lamprophyres have lower abundance of REE (∑REE = 524–1111 ppm) than the lamproites, although their patterns are similar and comparable to those of Krishna lamproites of southern India and West Kimberly lamproites of Australia.

In terms of incompatible element distribution patterns marked by negative Nb, Sr and P anomalies relative to REE, the Nuapada lamproites and lamprophyres are broadly similar to Krishna lamproites and West Kimberly lamproites (Fig. 11B). The Nuapada and Krishna rocks are additionally marked by depletion in Zr and Hf relative to REE which is absent in the West Kimberly lamproites. While the Nuapada and Krishna lamproites have similar degrees of depletion in Zr and Hf, the Nuapada lamprophyres exhibit somewhat higher degree of depletion in these elements.

References

Barnes, S.J. and Roedder, P.L. (2001) The range of spinel compositions in terrestrial mafic and ultramafic rocks. Jour. Petrol., v.42, pp.2279-2302.

Chalapathi Rao, N.V., Kamde, G., Kale, H.S. and Dongre, A. (2010) Petrogenesis of the Mesoproterozoic Lamproites from the Krishna Valley, Eastern Dharwar Craton, Southern India. Prec. Res., v.177, pp.103–130.

Dawson, J.B. and Stephens, W.E. (1975) Statistical classification of garnets from kimberlite and associated xenoliths. Jour. Geol., v.83, pp.589–607.

Fipke, C.E., Gurney, J.J. and Moore R.O. (1995) Diamond exploration techniques emphasizing indicator mineral geochemistry and Canadian examples. Geol. Surv. Canada Bull. 423.

Grütter, H.S., Gurney, J.J., Menzies, A.H. and Winter, F. (2004) An updated classification scheme for mantle-derived garnet, for use by diamond explorers. Lithos, v.77, pp.841–857.

Klemme, S. (2004) The influence of Cr on the garnet-spinel transition in the Earth's mantle: experiments in the system $MgO–Cr_2O_3–SiO_2$ and thermodynamic modeling. Lithos, v.77, pp.639–646.

Lehmann, B., Burgess, R., Frei, D., Belyatsky, B., Mainkar, D., Chalapathi Rao, N.V., Heaman, L.M. (2010) Diamondiferous kimberlites in central India synchronous with Deccan flood basalts. Earth Planet. Sci. Lett., v.290, pp.142–149.

Mitchell, R.H. and Bergman, S.C. (1991) Petrology of Lamproites. Plenum Press, New York, 447p.

Mukhopadhyay, P.K., Ghosh, S., Rath, S.C., Swain, R.B. and Shome, S. (2004) New finds of lamproite dykes in Nawapara district, Orissa. Indian Minerals, v.58, pp.183–196.

Reddy, T.A.K., Sridhar, M., Ravi, S., Chakravarthi, V. and Neelakantam, S. (2003) Petrography and geochemistry of the Krishna Lamproite Field, Andhra Pradesh. Jour. Geol. Soc. India, v.61, pp.131–146.

Shrivastava , S.K., Roy, A., Thakur, K.S., Muthuraman, K. and Khotpal, A.S. (2002). Discovery of lamproites by application of airborne geophysical techniques in eastern part of Bastar Craton. Geol. Surv. India Spl. Pub. No.75, pp.119–127.

Vijesh, V.K. (2010) Petrology of lamproites from the Krishna Lamproite Field, Andhra Pradesh. Unpub. M.Tech. (Geoexploration) thesis, IIT Bombay, 65p.